Journal of Hazardous Materials 196 (2011) 180–186

Contents lists available at SciVerse ScienceDirect

Journal of Hazardous Materials

journal homepage: www.elsevier.com/locate/jhazmat

Alkaline modified oil shale fly ash: Optimal synthesis conditions and preliminary tests on CO_2 adsorption

Janek Reinik[a,*], Ivo Heinmaa[a], Uuve Kirso[a], Toivo Kallaste[b], Johannes Ritamäki[e,g], Dan Boström[c], Eva Pongrácz[d,e], Mika Huuhtanen[e], William Larsson[g], Riitta Keiski[e], Krisztián Kordás[f,g], Jyri-Pekka Mikkola[g,h]

[a] National Institute of Chemical Physics and Biophysics, Akadeemia tee 23, EE-12618, Tallinn, Estonia
[b] Institute of Geology at Tallinn University of Technology, Ehitajate tee 5, EE-19086, Tallinn, Estonia
[c] Energy Technology and Thermal Process Chemistry ETPC, Department of Chemistry and the Department of Applied Physics and Electronics, Chemical-Biological Center, Umeå University, SE-90187, Umeå, Sweden
[d] Thule Institute, NorTech Oulu, University of Oulu, P.O. Box 8000, FI-90014 University of Oulu, Finland
[e] Mass and Heat Transfer Process Laboratory, P.O. Box 4300, FI-90014 University of Oulu, Finland
[f] Microelectronics and Materials Physics Laboratories, EMPART Research Group of Infotech Oulu, University of Oulu, P.O. Box 4500, FI-90014 Oulu, Finland
[g] Technical Chemistry, Department of Chemistry, Chemical-Biological Center, Umeå University, SE-90187, Umeå, Sweden
[h] Industrial Chemistry and Reaction Engineering, Process Chemistry Center, Åbo Akademi University, FI-20500, Åbo-Turku, Finland

ARTICLE INFO

Article history:
Received 18 July 2011
Received in revised form 1 September 2011
Accepted 4 September 2011
Available online 10 September 2011

Keywords:
Oil shale fly ash
Tobermorite synthesis
CO_2 thermo-gravimetric analysis

ABSTRACT

Environmentally friendly product, calcium–silica–aluminum hydrate, was synthesized from oil shale fly ash, which is rendered so far partly as an industrial waste. Reaction conditions were: temperature 130 and 160 °C, NaOH concentrations 1, 3, 5 and 8 M and synthesis time 24 h. Optimal conditions were found to be 5 M at 130 °C at given parameter range. Original and activated ash samples were characterized by XRD, XRF, SEM, EFTEM, ^{29}Si MAS-NMR, BET and TGA. Semi-quantitative XRD and MAS-NMR showed that mainly tobermorites and katoite are formed during alkaline hydrothermal treatment. Physical adsorption of CO_2 on the surface of the original and activated ash samples was measured with thermo-gravimetric analysis. TGA showed that the physical adsorption of CO_2 on the oil shale fly ash sample increases from 0.06 to 3–4 mass% after alkaline hydrothermal activation with NaOH. The activated product has a potential to be used in industrial processes for physical adsorption of CO_2 emissions.

1. Introduction

Oil shale processing residues pose a problem for the oil shale industry. Only in Estonia the power plants based on firing of oil shale produce 5–7 million tons of ash annually [1]. Oil shale ash is rendered so far mainly as a hazardous industrial waste because of high alkalinity and content of trace elements [2,3]. Less than 10 per cent of oil shale ash produced in Estonian power plants is utilized at the moment, mainly oil shale fly ash in cement industry [4]. However, the concentrations of heavy metals (e.g. Pb, Cd, Cr, Zn) in fly ash are higher than those in bottom ash and utilizing fly ash for construction materials can cause secondary pollution [5]. The focus of current work was to investigate possibilities for new industrial applications to oil shale fly ash.

Oil shale fly ash from Estonian power plants has a very high content of CaO (around 50%) and relatively high content of SiO_2 (ca. 22%) and Al_2O_3 (ca. 5%) by mass weight [4]. However, it is important to remember that the composition of oil shale fly ash vary, depending on combusted oil shale.

In the 1980s, German scientists invented a method for producing zeolites from coal fly ash [6]. Using the same hydrothermal activation method for Ca-rich oil shale ash, calcium–silica–aluminum (CSA) hydrates containing mainly tobermorites have been synthesized [7,8]. Tobermorites are core-binding phase in concrete [9] and can also be used as non-asbestos fire resistant materials [10]. Other uses of tobermorites include cation exchangers for cleaning low-level nuclear waste and adsorbents [11,12].

In the structure of tobermorites, the Al^{3+} ions are isomorphously substituted for Si^{4+} ions in tetrahedral sites, which in turn give to this structure a surplus negative charge. Na^+ ions are placed in the interlayer and compensate the deficient charge. Na^+ ions are mobile and easily pass into solution when substituted by heavy metal ions (Co^{2+}, Ni^{2+}, Zn^{2+}, etc.) [13,14]. Taking account the immobilizing properties of tobermorite structure in activated oil shale ash we assume that the release of heavy metals should diminish compared to original ash, witch in turn would make the product environmentally safer.

* Corresponding author. Tel.: +372 639 8356; fax: +372 670 3662.
E-mail addresses: jreinik@kbfi.ee, janek.reinik@kbfi.ee (J. Reinik).

0304-3894/$ – see front matter © 2011 Elsevier B.V. All rights reserved.
doi:10.1016/j.jhazmat.2011.09.006

Tobermorite occurs naturally, e.g. in Tobermory, Scotland [15] and tobermorites have been synthesized from a range of parent materials and industrial by-products [16–18]. Part of the work focused on finding optimal conditions for the synthesis of tobermorites from oil shale fly ash. The CSA hydrates from oil shale fly ash were synthesized at temperatures of 130 and 160 °C and NaOH concentrations of 1, 3, 5 and 8 M, respectively. The solid/solution ratio (350 g/dm^3) and reaction time (24 h) were constant throughout the experiments. The second objective of the work was to find a new application to synthesized product. We investigated the possibility of using the product for physical adsorption of CO_2. Fossil CO_2 emissions are considered a problem encountered in many industrial processes [19]. Adsorption is one of the more promising technologies for capturing CO_2 from exhaust gases, potentially avoiding the shortcomings of aqueous amine systems [20,21]. Several research studies have been made to evaluate the performance of various sorbents for CO_2 adsorption from flue gases, e.g. zeolites [22], carbon based materials (activated carbon and molecular sieve carbon) [23], hydrotalcite-like compounds and metal oxides (e.g. CaO and MgO) [24]; polymer based materials [25]; magnesium double salts, e.g. $K_2Mg(CO_3)_2$ [26] and also ionic liquids [27]. There are several ways to enhance the performance of an adsorbent, e.g. by means of chemical modification by addition of alkalis [28]. Moreover, several different CO_2 adsorption technologies are available, differing by the regeneration technology applied, such as pressure swing, vacuum swing, temperature swing, electric swing adsorption or combination of these regeneration technologies [29]. In the present work, laboratory scale tests of cyclic CO_2 adsorption on activated oil shale ash were conducted via thermal desorption to evaluate their repeated availability for CO_2 capture.

2. Materials and methods

Oil shale fly ash was collected from the 1st unit of electric precipitators of Estonian Power Plant's boiler (Narva Power Plants Ltd.) operating on circulating fluidized bed (CFB) principle. For the activation of oil shale ash the same reactor set-up and procedure was used as described in authors' previous work [8], except the activated product was washed only one time in distilled water.

X-ray diffraction patterns of original and activated ash samples were recorded with a HZG4 diffractometer (Freiberger Präzisionsmechanik, former DDR) with scintillation detector. Diffraction patterns of Co Ka were registered in the range of 5–65°2-theta.

Semi-quantitative XRD analyze of one activated oil shale ash sample (activated in 8 M NaOH solution at 160 °C for 24 h) was performed with Rietveld technique using DIFFRAC$_{plus}$ TOPAS R 2.1 (Bruker AXS GmnH, Karlsruhe, Germany, 2003). Structures from Inorganic Crystal Structure Database (Fachinformationszentrum, Karlsruhe, Germany, 2009) were used as starting models for the phases identified in the sample. Also, semi-quantitative XRD analysis was made using a Bruker d8 Advance instrument in $\theta - \theta$ mode, with an optical configuration consisting of a primary Göbel mirror and a Våntec-1 detector. Continuous scans were applied on the sample. By adding repeated scans, the total data collection time lasted for 6 h. The PDF2 databank (ICDD, Newtown Square, PA, 2004) together with Bruker software was used to analyze the diffraction patterns.

The chemical composition of major elements in original and activated ash samples was analyzed by the wavelength dispersive X-ray fluorescence (XRF) spectrometer S4 Pioneer (Bruker AXS GmbH) using integrated standardless evaluation technique (SPECTRA$_{plus}$).

^{29}Si MAS-NMR (Magic Angle Spinning-Nuclear Magnetic Resonance) spectra of original and activated samples was recorded on Bruker AMX-360 spectrometer at 8.5 T external magnetic field, using a bespoke MAS probe and 10 mm od zirconia rotors (rotation speed 5 kHz, simple 90° pulse excitation). About 400 accumulations with recycle time of 200 s were used to get reasonable signal to noise ratio.

Specific surface area was measured with Micrometrics TriStar 3000 sorptometer (Micrometrics Instrument Corp. USA). The samples (ca. 0.3 g) were degassed at temperature 120 °C for 5 h and before installing into sorptometer. Analysis adsorptive was N2 and bath temp. −196 °C. Isotherm data, BET surface area, *t*-plot, pore volumes were processed with TriStar 3000 v. 6.07 software.

SEM and EFTEM imaging for original ash and a characteristic sample activated in 4 M NaOH solution at temp. 130 °C were conducted with Zeiss FE-SEM Ultra Plus and Zeiss EFTEM (energy filtering transmission electron microscope, Carl Zeiss 201), respectively.

Thermo-gravimetric analysis for CO_2 adsorption was conducted with TGA Q 5000 (TA Instruments-Waters LLC, USA) supplied with Advantage for Q Series and Thermal Advantage (release 4.6.9) software. The method details were as follows:

1. The sample was dried at 120 °C for 100 min in N_2 environment.
2. The sample was equilibrated at 40 °C.
3. The gas flow was switched to a 70% CO_2 at flow rate 40 mL/min for 120 min.
4. The gas flow was reversed to pure N_2 and the sample was equilibrated at 115 °C and kept isothermal for 90 min.
5. The whole sequence was repeated.

In the thermo-gravimetric cyclic tests, the adsorption took place at the temperature of 40 °C (60 min) and desorption at the temperature of 115 °C (30 min). The cycle was repeated for 2 times.

3. Results

3.1. Nitrogen physisorption

For characterizing the product, the specific surface area was calculated from the N_2 absorption–desorption isotherm (P/P_0 = 0.025–0.999) using the B.E.T. equation [30]. The estimated constant *C* in BET equation was ranging from −6200 to 1000 in many sorption analyses, which means that in addition to mesopores the material also contained micropores. Therefore the *t*-plots and BJH cumulative pore specific surface area; cumulative pore volume and average pore diameter were also estimated (Table 1).

3.2. X-ray fluorescence (XRF) analysis

The chemical composition of original and activated ash (8 M NaOH solution at 160 °C) samples is presented in Table 2. The XRF analysis shows the increased concentration of Na^+ ions in the product. Excess of Na^+ can be removed by thorough washing of the activated material [31], which was not the objective of the work.

3.3. X-ray Roentgen diffraction (XRD) analysis

The X-Ray Roentgen diffraction patterns of the original and activated ash samples are presented in Fig. 1 and Fig. 2, respectively. The XRD analyses clearly demonstrate that the quartz in original ash is gradually converted into calcium–aluminum–silicate hydrates, depending on the NaOH concentration. Tobermorite 1 in Figs. 1 and 2 refers to reference pattern of $Ca_{2.25}[Si_3O_{7.5}(OH)_{1.5}]\cdot H_2O$ orthorhombic – *a* = 5.5860 | *b* = 3.6960 | *c* = 22.7790 [32] and tobermorite 2 refers to reference pattern $Ca_{4.5}Si_6O_{16}(OH)\cdot 5H_2O$ monoclinic – *a* = 6.7320 | *b* = 7.3690 | *c* = 22.6800 | gamma = 123.1800 [33].

Table 1
Results of nitrogen physisorption analysis.

Sample[a]	Surface area (m^2/g)			Pore volume (mm^3/g)		Average pore size (nm)	
	BET	*t*-plot micro-pore	BJH cumulative of pores between 1.7 and 100 nm	*t*-plot micro-pore	BJH cumulative of pores between 1.7 and 300 nm	BET	BJH
Original ash	6.3	0.77	7.3	0.35	36	23	20
1M130	38	5	38	2	143	15	15
3M130	59	14	58	7	264	18	18
5M130	61	14	61	7	269	18	18
8M130	70	18	67	9	360	21	21
1M160	58	11	59	5	236	16	16
3M160	50	11	50	5	196	16	16
5M160	47	10	45	5	250	22	22
8M160	58	14	57	7	310	21	22

[a] Sample name refers to activation conditions (1M130 means: ash sample activated in 1 M NaOH solution at the temperature of 130 °C, etc.).

Table 2
Chemical composition of major compounds in original fly ash and ash sample activated in 8 M NaOH solution at 160 °C.

Component	Original ash (wt%)	Activated ash, 8 M, 160 °C (wt%)
CaO	24	27
SiO_2	31	38
Al_2O_3	9.3	9.0
Fe_2O_3	3.9	4.5
MgO	3.2	4.6
Na_2O	0.1	2.5

The orthorhombic tobermorite suited best for all activated ash samples except one activated at temp 130 °C and in 8 M NaOH solution were monoclinic tobermorite achieved the best fit and also unidentified crystal phase was formed (see Fig. 1). The Si-external standard was inserted into sample for technical reason and gap in pattern 26–27° (2θ) of the original ash sample is a technical error.

The results of semi-quantitative analysis of mineral content of one activated oil shale fly ash sample are presented in Table 3. The activation conditions were: 8 M NaOH, at 160 °C for 24 h. The results show that the main mineral synthesized during the activation is tobermorite, whilst part of silica was also converted to katoite. Calcite and cancrinite are minerals originating from the native oil shale ash [34].

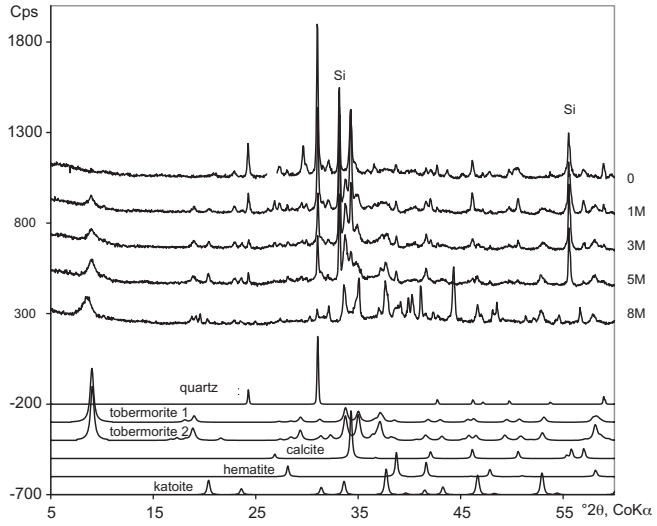

Fig. 1. XRD patterns of the original and activated ash samples, at different NaOH concentrations with reference patterns of major minerals. Temperature 130 °C; Si refers to internal silicon standard; tobermorite 1 and 2 refer to orthorhombic and monoclinic polytypes of 1.1 nm tobermorite, respectively.

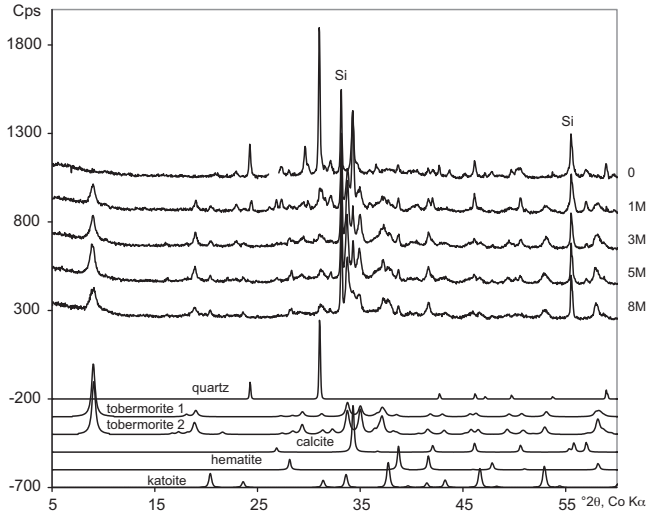

Fig. 2. XRD patterns of the original and activated ash samples at different NaOH concentrations with reference patterns of major minerals. Temperature 160 °C; Si refers to internal silicon standard; tobermorites 1 and 2 refer to orthorhombic and monoclinic polytypes of 1.1 nm tobermorite, respectively.

3.4. Magic angle spinning nuclear magnetic resonance (MAS-NMR) analysis

^{29}Si MAS-NMR spectra of the original and activated ash samples (at the temperatures of 130 and 160 °C) as well as the deconvolution of the spectra are presented in Fig. 3 and Fig. 4, respectively. The spectra of the original ash exhibit broad resonance in the chemical shift range from −80 to −110 ppm. This resonance can be assigned to the variety of silicon sites in the amorphous fly ash glass. The resonance lines at −71.5 and −107.3 ppm arise from belite (β-Ca_2SiO_4) [35] and quartz [36], respectively.

The chemical shift values of the ^{29}Si resonance of activated oil shale ash samples are typical to the silicon sites in silicate chains of tobermorites [37–40] or that of silicate hydrate gels [41–43]. The spectrums of activated oil shale ash samples present five resonance

Table 3
Semi-quantitative XRD mineral analysis of the oil shale sample activated in 8 M NaOH solution at the temperature of 160 °C.

Mineral	wt%
Tobermorite	75
Calcite	12
Katoite	9
Cancrinite	4

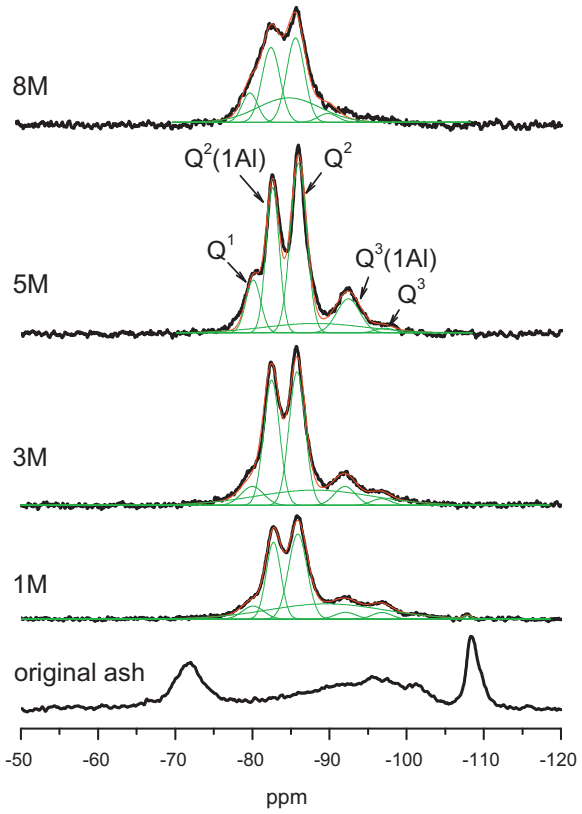

Fig. 3. MAS-NMR analyses of the original ash and samples activated at 130 °C in 1–8 M NaOH solution. Deconvolution with Gaussian curves.

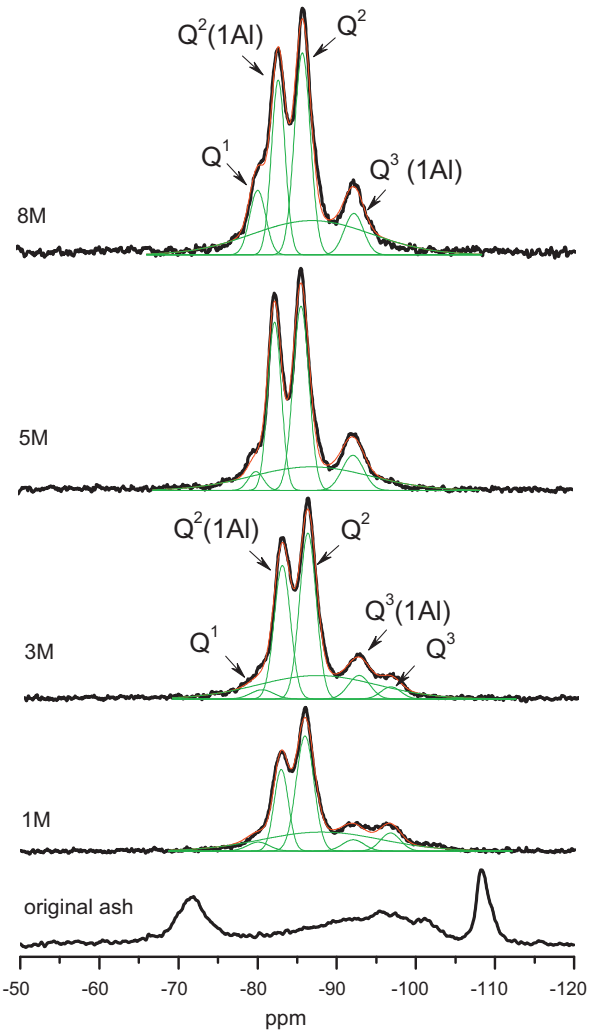

Fig. 4. MAS-NMR analyses of the original ash and samples activated at 160 °C in 1–8 M NaOH solution. Deconvolution with Gaussian curves.

lines at −80, −82.7, −85.8, −92 and −96.7 that can be assigned to the silicon sites Q^1, Q^2(1Al), Q^2(0Al), Q^3(1Al) and Q^3 of 1.1 nm tobermorite, respectively [37]. The site Q^1 is the silicon site at the end of the polymeric silicate chain in the SiO_4/AlO_4 tetrahedron chains ("dreierkette"), Q^2 is the silicon site in the chain middle groups, Q^2(1Al) is the chain middle group site where one of the two neighboring tetrahedra contains aluminum ion, Q^3 is the silicon site with three nearest neighbor SiO_4 tetrahedra, the branching tetrahedron which links together two chains, and Q^3(1Al) is the site, where one of the three nearest neighbor tetrahedra contains an Al ion [8]. The best fit was achieved when we added underneath of the well-resolved lines a broad Gaussian background line (Q^x) with center position of the peak at −89.5 ppm, which arises from silicon configurations of amorphous calcium–silicate hydrate phase.

Some quantitative characteristics of ash samples can be obtained from the deconvolution of the ^{29}Si MAS-NMR spectra by Gaussian lines using relative intensities of the ^{29}Si lines in Table 4. The mean length n of SiO_4/AlO_4 chains and the ratio of Al/Si were evaluated from the formulas presented in Refs. [8] and [43].

The data reveals that the average chain length of activated oil shale ash remains constant at the temperature of 130 °C and increases with increasing temperature, except for sample activated in 8 M NaOH solution. Ratio of aluminum to silicon is not dependent on reaction conditions and remains in between 0.12 and 0.19.

3.5. Scanning electron and transmission electron microscopy (SEM-TEM) analysis

Imaging results of scanning electron and transmission electron microscopes for the original ash vs. a sample activated in 4 M NaOH solution at 130 °C are presented in Figs. 5 and 6, respectively.

Table 4
Relative intensities of Gaussian lines in ^{29}Si MAS-NMR spectras with center position of the peak in ppm. I_1–I_3 are the intensities of lines assigned to silicon sites Q^1–Q^3, respectively. I_x is the intensity of the broad background line arising from amorphous silicon sites.

Ash Sample	I_1 −80	I_2(1Al) −82.7	I_2 85.8	I_3(1Al) −92	I_3 −96.7	I_x −89.5	n	Al/Si
1M130	0.06	0.15	0.27	0.03	0.02	1.90	21	0.14
3M130	0.09	0.30	0.34	0.02	0.02	1.94	21	0.19
5M130	0.11	0.24	0.43	0.17	0.02	0.90	21	0.12
8M130	0.06	0.20	0.23	0.03	0	0.90	21	0.19
1M160	0.04	0.15	0.32	0.05	0.06	2.36	36	0.12
3M160	0.04	0.31	0.41	0.10	0.04	2.92	55	0.17
5M160	0.04	0.27	0.41	0.14	0	2.95	53	0.16
8M160	0.11	0.21	0.34	0.10	0	3.22	17	0.14

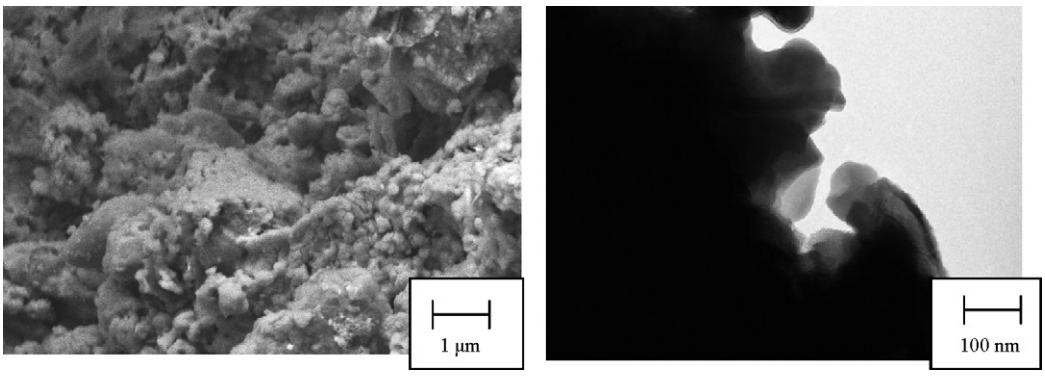

Fig. 5. SEM (left) and TEM (right) images of the native oil shale fly ash.

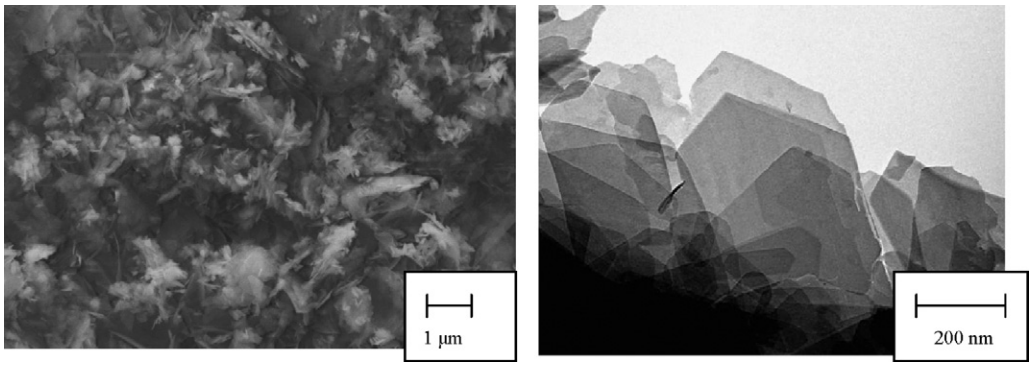

Fig. 6. SEM (left) and TEM (right) images of the oil shale fly ash sample activated in 4 M NaOH solution at 130 °C.

SEM analysis demonstrated that the original ash had smooth surface structure and particles had spherical shapes (Fig. 5). The texture of the activated ash is more obscure and TEM image confirms that crystal morphologies are formed on the surface (Fig. 6).

3.6. Thermo-gravimetric analysis (TGA)

The results of CO_2 adsorption on the surface of original and some samples of activated fly ash are presented in Fig. 7 and Fig. 8. The original oil shale ash adsorbs 0.03–0.06 mass% of CO_2 at 40 °C during 120 min period. The CO_2 adsorption capacity of alkaline treated oil shale ash (3 M NaOH solution, at 160 °C) is up to 4.4 mass% under similar conditions.

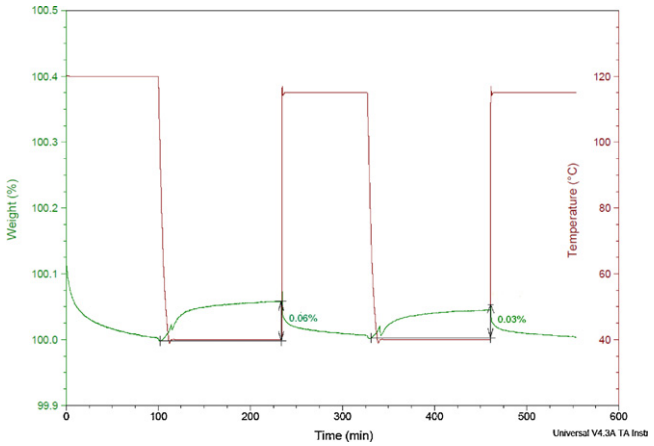

Fig. 7. Thermo-gravimetric analysis of CO_2 adsorption onto original oil shale fly ash sample.

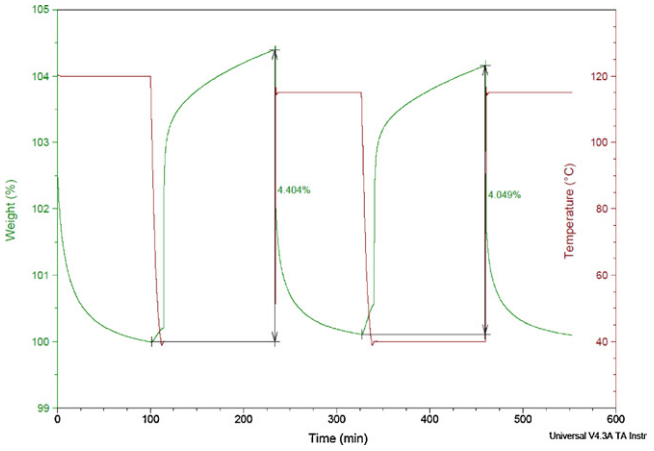

Fig. 8. Thermo-gravimetric analysis of CO_2 adsorption onto ash sample activated in 3 M NaOH solution at 160 °C.

Results of CO_2 adsorption onto original and selected ash samples at temperature 40 °C and 120 min period are presented in Table 5. According to Table 5, the samples activated at temperature 160 °C adsorb 2–3 times more CO_2 than those activated at temperature 130 °C.

Table 5
Maximum physical adsorption of CO_2 onto selected ash samples at temperature 40 °C during 120 min.

Sample	CO_2 adsorption wt%
Original ash	0.06
1M130	1.8
8M130	1.3
5M160	3.7
3M160	4.4

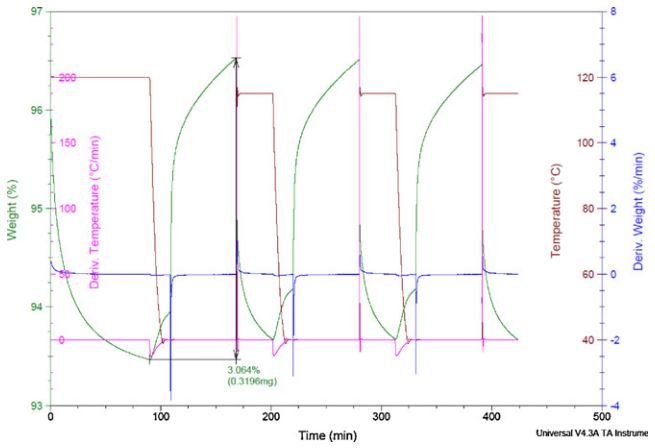

Fig. 9. Cyclic thermo-gravimetric analysis of CO_2 adsorption onto ash sample activated in 5 M NaOH solution at 160 °C.

According to cyclic adsorption test with ash sample activated in 5 M NaOH solution at 160 °C, the adsorption capacity of the activated ash sample diminishes less than 5% after two adsorption/thermal desorption cycles (Fig. 9).

4. Discussions and conclusions

Synthetic calcium–silica–aluminum hydrates, mainly 1.1 nm tobermorite and katoite, were produced from oil shale fly ash at a laboratory scale. Reaction parameters were alkali concentration and temperature whilst solid/liquid ratio and reaction time were kept constant. XRD and MAS-NMR analysis demonstrated that formation of synthetic hydrates and dissolution of silica depends positively on both alkali concentration and reaction temperature, at given range (1–8 M NaOH solution concentration; 130 °C and 160 °C). The highest yield of 1.1 tobermorite was obtained with 5 M NaOH solution at the temperature of 160 °C (Fig. 10).

During the activation of oil shale ash specific surface area (m^2/g) increased over 10 times and the cumulative volume of pores (mm^3/g) 100 times, which gives us indication of the formation of micropores in tobermorite structure. Some dependence of specific surface increase on alkali concentration was observed in the samples activated at 130 °C.

Semi-quantitative XRD analysis illustrated that minerals synthesized during oil shale activation were tobermorite (75 mass%) and katoite (9 mass%). According to MAS-NMR analysis, the tobermorite can be assigned to 1.1 nm tobermorite.

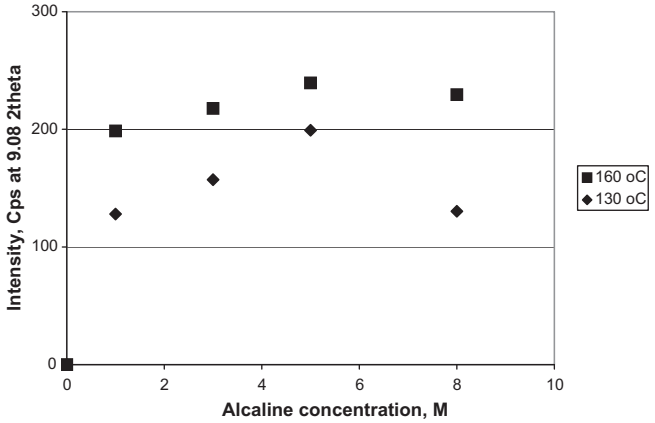

Fig. 10. XRD peak intensities of tobermorite at 9.08θ, at different reaction conditions.

The results of TGA show that the alkaline treatment of oil shale ash increases the CO_2 adsorption capacity and is dependent on reaction temperature. The CO_2 adsorption tests were carried out in dry conditions. The residual NaOH in activated materials plays role in CO_2 adsorption under humid conditions. Therefore we assume that the main cause of increase in CO_2 adsorption capacity is the formation of synthetic minerals, which leads to increased specific area and pore volumes in product. The adsorption capacity of alkali-treated (3–4 mass%) ash is coherent with the results obtained from other CO_2 adsorption research [44]. Furthermore, the cyclic test for CO_2 adsorption/thermal desorption demonstrated that the activated oil shale ash can be regenerated for multiply adsorption–desorption cycles for CO_2 capture. Future study will address CO_2 adsorption onto activated oil shale ash in a pilot scale industrial process. Also for other applications, the leaching test of original and activated product will be made in order to assess the trend on bioavailability of heavy metals from the native and treated oil shale fly ash.

Acknowledgments

This work was supported by grant SF 0690001s09 from the Estonian Ministry of Education and Research. In Sweden, the Bio4Energy program, Knut and Alice Wallenberg Foundation as well as Kempe Foundations are acknowledged. Also, the Micre (Micro Energy to Rural Enterprise) project under the auspices of the Northern Periphery Program by the EU is acknowledged.

References

[1] R. Mõtlep, T. Sild, E. Puura, K. Kirsimäe, Composition, diagenetic transformation and alkalinity potential of oil shale ash sediments, J. Hazard. Mater. 184 (2010) 567–573.
[2] E. Häsänen, L. Aunela-Tapola, V. Kinnunen, K. Larjava, A. Mehtonen, T. Salmikangas, J. Leskelä, J. Loosaar, Emission factors and annual emissions of bulk and trace elements from oil shale fueled power plants, Sci. Total Environ. 198 (1997) 1–12.
[3] M. Laja, G. Urb, N. Irha, J. Reinik, U. Kirso, Leaching behavior of ash fractions from oil shale combustion by fluidized bed and pulverized fuel processes, Oil Shale 22 (2005) 453–465.
[4] A. Ots, Oil Shale Fuel Combustion, Tallinna Raamatutrükikoda, Tallinn, 2006.
[5] J. Luan, A. Li, T. Su, X. Cui, Synthesis of nucleated glass-ceramics using oil shale fly ash, J. Hazard. Mater. 173 (2010) 427–432.
[6] H. Höller, U. Wirsching, Zeolites formation from fly ash, Fortschr. Miner. 63 (1985) 21–43.
[7] R.A. Shawabkeh, Synthesis and characterization of activated carbo-aluminosilicate material from oil shale, Microporous Mesoporous Mater. 75 (2004) 107–114.
[8] J. Reinik, I. Heinmaa, J.P. Mikkola, U. Kirso, Hydrothermal alkaline treatment of oil shale ash for synthesis of tobermorites, Fuel 86 (2007) 669–676.
[9] I.G. Richardson, The calcium silicate hydrates, Cem. Concr. Res. 38 (2008) 137–158.
[10] X. Querol, N. Moreno, J.C. Umaña, A. Alastuey, E. Hernández, A. López-Soler, F. Plana, Synthesis of zeolites from coal fly ash: an overview, Int. J. Coal Geol. 50 (2002) 413–423.
[11] N.J. Coleman, Interactions of Cd(II) with waste-derived 11 Å tobermorites, Sep. Purif. Technol. 48 (2006) 62–70.
[12] R.A. Shawabkeh, Equilibrium study and kinetics of Cu^{2+} removal from water by zeolite prepared from oil shale ash, Process Saf. Environ. Prot. 87 (2009) 261–266.
[13] R. Siauciunas, V. Janickis, D. Palubinskaite, R. Ivanauskas, The sorption properties of tobermorite modified with Na^+ and Al^{3+} ions, Ceramics – Silikáty 48 (2004) 76–82.
[14] M. Miyake, S. Komarneni, R. Roy, Kinetics equilibria and thermodynamics of ion exchange in substituted tobermorites, Mater. Res. Bull. 24 (1989) 311–320.
[15] M.F. Heddle, Preliminary notices on substances which may prove to be new minerals, Mineral. Mag. 4 (1882) 117–123.
[16] N.J. Coleman, Synthesis, structure and ion exchange properties of 11 Å tobermorites from newsprint recycling residue, Mater. Res. Bull. 40 (2005) 2000–2013.
[17] Z. Yao, C. Tamura, M. Matsuda, M. Miyake, Resource recovery of waste incineration fly ash: synthesis of tobermorite as ion exchanger, J. Mater. Res. 14 (1999) 4437–4442.
[18] N.J. Coleman, C.J. Trice, J.W. Nicholson, 11 Å tobermorite from cement bypass dust and waste container glass: a feasibility study, Int. J. Miner. Process. 93 (2009) 73–78.

[19] H.J. Leimkühler, Managing CO_2 Emissions in the Chemical Industry, Wiley-VCH, Weinheim, 2010.
[20] T.C. Drage, K.M. Smith, C. Pevida, A. Arenillas, C.E. Snape, Development of adsorbent technologies for post-combustion CO_2 capture, Energy Procedia 1 (2009) 881–884.
[21] M. Wilson, P. Tontiwachwuthikul, A. Chakma, R. Idem, A. Veawab, A. Aroonwilas, D. Gelowitz, J. Barrie, C. Mariz, Test results from a CO_2 extraction pilot plant at boundary dam coal-fired power station, Energy 29 (2004) 1259–1267.
[22] R.V. Siriwardane, M.S. Shen, E.P. Fisher, Adsorption of CO_2 on zeolites at moderate temperatures, Energy Fuels 19 (2005) 1153–1159.
[23] M. Pellerano, P. Pré, M. Kacem, A. Delebarre, CO_2 capture by adsorption on activated carbons using pressure modulation, Energy Procedia 1 (2009) 647–653.
[24] Z. Yong, V. Mata, A.E. Rodrigues, Adsorption of carbon dioxide at high temperature—a review, Sep. Purif. Technol. 26 (2002) 195–205.
[25] C. Lu, F. Su, S.C. Hsu, W. Chen, H. Bai, J.F. Hwang, H.H. Lee, Thermodynamics and regeneration of CO_2 adsorption on mesoporous spherical-silica particles, Fuel Process. Technol. 90 (2009) 1543–1549.
[26] R. Singh, M.K. Ram Reddy, S. Wilson, K. Joshi, J.S. Diniz da Costa, P.A. Webley, High temperature materials for CO_2 capture, Energy Procedia 1 (2009) 623–630.
[27] F. Karadas, M. Atilhan, S. Aparicio, Review on the use of ionic liquids (ILs) as alternative fluids for CO_2 capture and natural gas sweetening, Energy Fuels 24 (2010) 5817–5828.
[28] J. Zhang, R. Singh, P.A. Webley, Alkali and alkaline-earth cation exchanged chabazite zeolites for adsorption based CO_2 capture, Microporous Mesoporous Mater. 111 (2008) 478–487.
[29] M. Erikson, R. Backman, Post Combustion CO_2 Capture in the Swedish Lime and Cement Industries, Print & Media, Umeå Universitet, Umeå, 2009.
[30] S. Brunauer, P.H. Emmet, E. Teller, Adsorption of gases in multimolecular layers, J. Am. Chem. Soc. 60 (1938) 309–319.
[31] J. Reinik, I. Heinmaa, J.P. Mikkola, U. Kirso, Synthesis and characterization of calcium-alumino-silicate hydrates from oil shale ash – towards industrial applications, Fuel 87 (2008) 1998–2003.
[32] S.A. Hamid, The crystal structure of the 11 Å natural tobermorite $Ca_{2.25}(Si_3O_{7.5}(OH)_{1.5})(H_2O)$, Z. Kristallogr. 154 (1981) 189–198.
[33] S. Merlino, E. Bonaccorsi, T. Armbruster, The real structure of tobermorite 11 Å: normal and anomalous forms, OD character and polytypic modifications, Eur. J. Mineral. 13 (2001) 577–590.
[34] A. Paat, R. Traksmaa, Investigation of the mineral composition of Estonian oil-shale ash using X-ray diffractometry, Oil Shale 19 (2002) 373–386.
[35] M. Mägi, E. Lippmaa, A. Samoson, G. Engelhardt, A.R. Grimmer, Solid state high-resolution silicon-29 chemical shifts in silicates, J. Phys. Chem. 88 (1984) 1518–1522.
[36] E. Lippmaa, M. Mägi, A. Samoson, G. Engelhardt, A.R. Grimmer, Structural studies of silicates by solid state high resolution ^{29}Si NMR, J. Am. Chem. Soc. 102 (1980) 4889–4893.
[37] W. Wieker, A.R. Grimmer, A. Winkler, M. Mägi, M. Tarmak, E. Lippmaa, Solid-state high-resolution ^{29}Si NMR spectroscopy of synthetic 14 Å, 11 Å and 9 Å tobermorites, Cem. Concr. Res. 12 (1982) 333–339.
[38] S. Komarneni, R. Roy, D.M. Roy, C.A. Fyfe, G.J. Kennedy, A.A. Bothner-By, J. Dadok, A.S. Chesnick, ^{27}Al, ^{29}Si magic angle spinning nuclear magnetic resonance spectroscopy of Al-substituted tobermorites, J. Mater. Sci. 20 (1985) 4209–4214.
[39] S. Komarneni, M. Tsuji, Selective cation exchange in substituted tobermorites, J. Am. Ceram. Soc. 72 (1989) 1668–1674.
[40] T. Maeshima, H. Noma, M. Sakiyama, T. Mitsuda, Natural 1.1 and 1.4 nm tobermorites from Fuka, Okayama, Japan: chemical analysis, cell dimensions, ^{29}Si NMR and thermal behavior, Cem. Concr. Res. 33 (2003) 1515–1523.
[41] I.G. Richardson, A.R. Brough, R. Brydson, G. Groves, C.M. Dobson, Location of aluminum in substituted calcium silicate hydrate (C-S-H) gels as determined by ^{29}Si and ^{27}Al NMR and EELS, J. Am. Ceram. Soc. 76 (1993) 2285–2288.
[42] A.R. Brough, C.M. Dobson, I.G. Richardson, G.W. Groves, Application of selective ^{29}Si isotopic enrichment to studies of the structure of calcium silicate hydrate (C-S-H) gels, J. Am. Ceram. Soc. 77 (1994) 593–596.
[43] M.D. Andersen, H.J. Jakobsen, J. Skibsted, Characterization of white Portland cement hydration and the C-S-H structure in the presence of sodium aluminate by ^{27}Al and ^{29}Si MAS NMR spectroscopy, Cem. Concr. Res. 34 (2004) 857–868.
[44] M. Bhagiyalakshmi, L.J. Yun, R. Anuradha, H.T. Jang, Utilization of rice husk ash as silica source for the synthesis of mesoporous silicas and their application to CO_2 adsorption through TREN/TEPA grafting, J. Hazard. Mater. 175 (2010) 928–938.